Impacts of Phosphate Amendments on Lead Biogeochemistry at a Contaminated Site

XINDE CAO,[†] LENA Q. MA,*[,†] MING CHEN,[‡] SATYA P. SINGH,[§] AND WILLIE G. HARRIS[†]

Soil and Water Science Department, University of Florida, Gainesville, Florida 32611, Everglades Research and Education Center, University of Florida, Belle Glade, Florida 33430, and Department of Geological Sciences, University of Saskatchewan, Saskatoon, Saskatchewan, Canada S7J 2A6

Soil amendments can be used to cost-effectively reduce the bioavailability and mobility of toxic metals in contaminated soils. In this study a field demonstration was conducted at a Pb-contaminated site to evaluate the effectiveness of P-induced Pb immobilization. Phosphate was applied at a 4.0 molar ratio of P to Pb with three treatments: T1, 100% of P from H_3PO_4; T2, 50% P from H_3PO_4 + 50% P from $Ca(H_2PO_4)_2$; and T3, 50% P from H_3PO_4 + 5% phosphate rock. Phosphate amendments effectively transformed soil Pb from the nonresidual (sum of exchangeable, carbonate, Fe/Mn, and organic) to the residual fraction, with residual Pb increase by 19−48% for T1, 22−50% for T2, and 11−55% for T3, respectively. Lead immobilization was attributed to the P-induced formation of chloropyromorphite [$Pb_{10}(PO_4)_6Cl_2$], which was identified in the surface soil, subsurface soil, and plant rhizosphere soil. Occurrence of chloropyromorphite was evident 220 days after P addition for T1 and T2 treatments and 330 days for T3. Visual MINTEQ model and activity-ratio diagram indicated that lead phosphate minerals controlled Pb^{2+} activities in the P-treated soils. Phosphate treatments significantly reduced Pb translocation from the roots to the shoots in the St. Augustine grass (*Stenotaphrum secundatum*), possibly via the formation of chloropyromorphite on the cell walls of roots. This field observation suggested that P amendments are efficient in reducing Pb mobility via in situ formation of insoluble chloropyromorphite minerals at a field setting. Lead immobilization shows a long-term stability. A mixture of H_3PO_4 and phosphate rock yields the best overall results for in situ Pb immobilization, with less soil pH change and less P leaching. Application of combined H_3PO_4 with phosphate rock may provide an effective alternative to the current phosphate remediation technologies for contaminated soils.

Introduction

Biogeochemical cycling of metals in the environment depends on their chemical forms. Significant fractions of metals in contaminated soils are often present in the potentially bioavailable fractions (*1*). Thus, considerable effort has been focused on developing cost-effective technologies to control metal bioavailability and mobility in contaminated soils. Amendment-induced changes in metal biogeochemistry may significantly lower metal solubility and their ecotoxicity, providing a strategy for remediation of metal contaminated soils.

Phosphate has been shown to effectively immobilize Pb in contaminated soils (*2*−*8*). Its effectiveness is based on P-induced conversion of reactive Pb into less labile lead phosphate. In the presence of adequate P, lead-phosphates are at least 44 orders of magnitude less soluble than galena (PbS), anglesite ($PbSO_4$), cerussite ($PbCO_3$), and litharge (PbO), which are common Pb minerals in contaminated soils (*9, 10*). Natural lead-phosphate minerals have been identified in contaminated soils (*10*−*13*). In light of their intrinsically low solubilities, efforts have been made to form lead-phosphates in lead-contaminated soils through P addition. Highly soluble forms of P (e.g. Na_2HPO_4 or KH_2PO_4) can significantly reduce Pb bioavailability (*14, 15*) via formation of lead-phosphate (*4*). Ma et al. (*16*) showed that less soluble hydroxyapatite [$Ca_{10}(PO_4)_6(OH)_2$] effectively immobilizes aqueous Pb via formation of hydroxypyromorphite. Phosphate rock [PR, primarily $Ca_{10}(PO_4)_6F_2$] is also shown to effectively immobilize Pb from aqueous solution and lead-contaminated soils (*6*). The main mechanism of Pb immobilization is via dissolution of PR and subsequent precipitation of pyromorphite-like minerals [$Pb_{10}(PO_4)_6X_2$, X = F, Cl, Br, OH] (*16*). Direct evidence for the formation of pyromorphite in Pb contaminated soils upon P addition has been reported using X-ray diffraction (XRD), scanning electron microscopy (SEM), atomic force microscopy (AFM), and extended X-ray absorption fine structure spectroscopy (EXAFS) techniques (*7, 9, 17, 18*).

If sufficient soluble P is provided, dissolution of solid-phase soil Pb is the rate-limiting step for formation of pyromorphite-like minerals (*7, 8*). Laperche et al. (*9*) reacted hydroxyapatite with litharge/massicot (PbO) and cerussite at pH 5−8 and found that conversion to hydroxypyromorphite was the fastest at pH = 5. Thus, acidity of the soil is important in Pb immobilization using phosphate amendment. Adding H_3PO_4 would lower soil pH to facilitate dissolution of soil Pb and increase activity of soluble P to enhance pyromorphite formation. Application of H_3PO_4 to contaminated soils has been shown to stabilize and reduce leaching of Pb (*5, 8*). Insoluble chloropyromorphite was identified in H_3PO_4 treated Pb-contaminated soils and in mine tailings (*19, 20*). Unfortunately, treatments with highly soluble H_3PO_4 may increase the risk of P-induced eutrophication (*4*). Less soluble P such as PR and apatite may reduce such a risk in addition to supply a continued source of P in the soil to react with Pb. Hence, application of combined H_3PO_4 with less soluble P sources may be a good choice. However, information for this method is lacking.

In addition, since in situ Pb immobilization does not change total Pb concentration in a soil, it is important to obtain information on the time required for reducing soil Pb bioavailability after P application as well as the long-term stability of Pb immobilization. With time, continued P consumption by plants may cause decomposition of the lead

* Corresponding author phone: (352)392-9063; fax: (352)392-3902; e-mail: lqma@ufl.edu. Corresponding author address: Soil and Water Science Department, University of Florida, P.O. Box 110290, Gainesville, FL 32611-0290.

[†] Soil and Water Science Department, University of Florida.

[‡] Everglades Research and Education Center, University of Florida.

[§] University of Saskatchewan.

10.1021/es020697j CCC: $22.00
Published on Web 11/13/2002

TABLE 1. Selected Physical and Chemical Properties of the Soil and Phosphate Rock[a]

	pH[b]	CEC[c] cmol kg^{-1}	% OM[d]	% sand	% silt	% clay	g kg^{-1} P_T[e]	g kg^{-1} Pb_T	g kg^{-1} Cu_T	g kg^{-1} Zn_T
soil	6.95 ± 0.19	5.75 ± 0.85	3.91 ± 0.90	87.7 ± 1.37	9.0 ± 1.58	3.35 ± 0.54	0.89 ± 0.16	11.6 ± 1.57	2.64 ± 0.11	1.95 ± 0.83
PR[f]	7.10 ± 0.31	ND[g]	ND	ND	ND	ND	143 ± 9.87	BDL[h]	BDL	0.054 ± 0.004

[a] Data represent an average of twelve replicates with a standard deviation. [b] pH was determined with a 1:1 ratio of soil/water. [c] Cation exchange capacity. [d] Organic matter. [e] Total concentration. [f] Phosphate rock. [g] Not determined. [h] Below detection limit (Pb < 0.25 mg kg^{-1}, Cu < 0.20 mg kg^{-1}).

phosphate compounds previously formed. Similarly, changes in soil biogeochemistry may affect the permanence of the P-induced modifications.

In the present study, a field demonstration of Pb-immobilization using H_3PO_4 combined with $Ca(H_2PO_4)_2$ or phosphate rock amendments was conducted at a lead-contaminated urban site. The objectives of this research were (1) to demonstrate P-induced phytoavailability and mineralogical changes of Pb at a contaminated site; (2) to apply geochemical modeling to predict minerals controlling Pb activity in P-treated soils; (3) to compare the effects of different P sources on in situ Pb immobilization; and (4) to assess long-term stability of in situ immobilization of lead at a contaminated site.

Materials and Methods

Site Characterization. The demonstration site is located in northwest of Jacksonville, Florida. It is a nearly-level area of ~4100 m^2 (71.4 m × 57.3 m) with surface runoff in a west to southwesterly direction. The site is used for battery recycling and salvage yard with discharge of waste oil during 1940s. The site map, soil characteristics, pollutants of concern, and contamination distribution were reported in Cao et al. (*21*). Overall, the soil is slightly alkaline and mainly contaminated with Pb from both spatial and vertical dimension. Cerussite was the predominant form of Pb at the site. The hotspot is centered in the north-central part of the site. For other metals (Cu and Zn), their concentrations also remained 10−100 times higher compared to their normal concentrations found in Florida soils (*21*).

Experimental Plot Establishment. Four tested plots were established in the north-central (hotspot) part of the site. Selected soil properties at tested plots are given in Table 1. Each plot consisted of an area of 4 m^2, which was isolated by high-density polyethylene geomembrane liner of 2.5-mm in thickness to prevent flooding out of or into the plots. The plots were separated 1.5-m in distance from each other to avoid possible inter-plot contamination. Phosphate amendments were applied to three plots (T1, T2, and T3) with three treatments, respectively, at a 4 molar ratio of P to Pb based on the results of our preliminary test (*21*). The total amount of P added was calculated for the surface soil of 0−20 cm depth. To pre-acidify the soil, half of the P was first applied to the three plots on 02/17/2000 as H_3PO_4 by mixing it with 25 L of water and spraying it uniformly in each area (liquid-to-solid ratio L/S = 0.03). The plots were then covered with a plastic sheet to maintain the moisture content of the surface layers and to prevent leaching from rainfall. On 03/27/2000, 40 days after the first application, the second half of the P amendments was applied as H_3PO_4 in T1, $Ca(H_2PO_4)_2$ in T2 and phosphate rock (PR) in T3 by uniformly mixing them with a shovel to a depth of 20 cm. This is a passive mixing approach with minimum site disturbance compared to the large-scale field operation using machinery such as plus mills. The plot without P treatment was set as the control (T0). After the second P application, the plots were exposed to rainfall. St. Augustine grass (*Stenotaphrum secundatum*) was predominantly and naturally growing at the tested site. After P application, aboveground biomass regenerated from the roots. Phosphate rock used in this research was obtained from Occidental Corp (White Spring, FL; Table 1). It consists mainly of $Ca_{10}(PO_4)_6F_2$ with substantial CO_3^{2-} substitution in the structure (*6*). In our study, low concentrations of Pb and other metals were detected in the PR (Table 1).

Soil and Plant Sampling. Triplicates of soil samples were collected from each plot at 6 depth intervals of 0−10, 10−20, 20−30, 30−40, 40−60, and 60−80 cm on 7, 50, 130, 220, 330, and 480 days after the first P application. All soil samples were air-dried and passed through a 2-mm sieve, followed by HNO_3/H_2O_2 hot block digestion procedure (USEPA Method 3050a) for metal analysis. St. Augustine grass was collected and separated into roots and aboveground biomass. After being rinsed with deionized water, the aboveground biomass was oven-dried at 65 °C for 4 d and digested with USEPA Method 3050a, while roots were cleaned ultrasonically in deionized water to completely remove soils and then oven dried for digestion. Rhizosphere soils obtained by ultrasonifying roots were collected on a 0.2 μm membrane filter.

Soil Pb Fractionation. A modified sequential extraction procedure developed by Tessier (*22*) was used to separate soil Pb into different fractions. The scheme operationally separated Pb into the following fractions: water soluble and exchangeable (WE), carbonate (CB), Fe−Mn oxides (FM), organic (OC), and residual (RS) fractions. The residual fraction was determined after digestion using HNO_3/H_2O_2 (USEPA Method 3050a). To ensure quality, a comparison of summed fractions using Standard Reference Material (SRM2710) was compared to total Pb content via digestion using HNO_3/H_2O_2. The summed fractions averaged 103 ± 10% of the total Pb, indicating a good recovery using the fractionation scheme.

Lead Activity Modeling. Twenty milliliters of 0.01 M $Ca(NO_3)_2$ was added to 2 g dried soils from the control and P-treated plots. The mixtures were shaken for 24 h at 25 °C. After the equilibration period, the soil solutions were filtered with 0.45 μm membrane followed by pH determination and anion concentration analysis. Remaining portions were acidified to pH < 2 for metal analysis. The results of ion analysis were then put into the chemical equilibrium speciation model Visual MINTEQ (*23*) to calculate Pb species activity in soil solution. An activity ratio diagram of Pb was developed on the basis of dissolution equilibrium of Pb minerals. Chemical speciation data obtained from Visual MINTEQ were plotted on the diagram to identify minerals potentially controlling Pb solubility.

X-ray Diffraction and Electron Microscopy Analysis. Soil clay fractions were separated from all soil samples by wet centrifugation (*24*) and analyzed using XRD. Samples were scanned from 2 to 60° 2θ with Cu Kα radiation on a computer-controlled diffractometer equipped with stepping motor and graphite crystal monochromator. Selected samples analyzed by XRD were further examined by using a scanning electron microscopy (SEM, JSM-6400/TN500, JEOL, USA), equipped with an energy-dispersive X-ray elemental spectrometer (EDS). Part of the fresh root samples collected 480 days after P application from T2 plot was examined with a transmission electron microscope (TEM Philips 420EM) coupled with EDS.

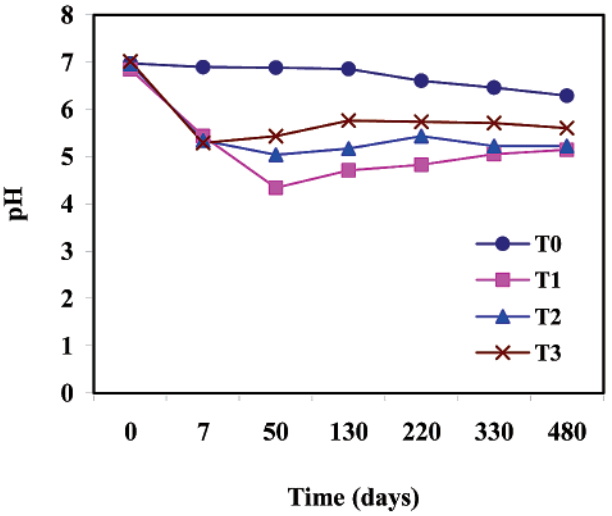

FIGURE 1. pH changes in the surface soils (0−10 cm) in the tested plots as a function of time. T0, control; T1, H_3PO_4; T2, H_3PO_4 + $Ca(H_2PO_4)_2$; T3, H_3PO_4 + phosphate rock.

Preparation of the root sections followed the procedure developed by Laperche et al. (*25*).

Chemical Analysis. Soil organic matter was determined using the Walkley-Black procedure (*26*). Cation exchangeable capacity (CEC) was examined using the method of Rhoades (*27*). Total phosphorus was measured colorimetrically with a Shimadzu 160U spectrometer using the molybdate/ascorbic acid method (*28*). Anions (Cl, Br, F, SO_4, and PO_4) were determined by using ion chromatography (Waters 2690 Separations Module, Waters Corporation, USA). Metals (Pb, Cu, Zn, etc.) were determined by using inductively coupled plasma spectrometry (Thermo Jarrell Ash ICAP 61-E, Franklin, MA) and by using graphite furnace atomic absorption spectrometry (Perkin-Elmer SIMMA 6000, Perkin-Elmer Corp., Norwalk, CT). Elemental analysis followed EPA approved QA/QC plan with a blank, a duplicate, a spike and a SRM analysis every 20 samples. Quality control samples included Standard Reference Materials of soil (SRM 2709 San Joaquin Soil, 2710 Montana Soil) and plant (1547 Peach Leaves) (U.S. Department of Commerce National Institute of Standards and Technology, Gaithersburg, MD 20899). Satisfactory precision and accuracy were required to be within ±20% and between 85 and 120%, respectively.

Data Analysis. All results are expressed as an average of triplicates with standard deviation, and treatment effects were determined by analysis of variance according to general linear model procedure of the Statistical Analysis System (SAS Institute Inc.). Significance was tested at the 0.01 and 0.05 probability levels.

Result and Discussion

Effects on Soil pH. As expected, application of P amendments impacted the pH of this sandy soil with relatively low buffer capacity (>89% sand, Table 1). Soil pH was reduced in all P-treated plots due to addition of H_3PO_4 (Figure 1). Among all treatments, T1 produced the greatest decrease in soil pH, while T3 produced the least ($p < 0.05$). Application of $Ca(H_2PO_4)_2$ or phosphate rock combined with H_3PO_4 maintained a soil pH slightly higher than H_3PO_4 alone. Soil pH in the T3 plot decreased to its lowest point (pH 5.2) on day 7 after the treatment, then gradually recovering to finally stabilize on day 130. For the T1 and T2 treatments, soil pH reached its lowest point on day 50, and stabilized on day 220 and 330, respectively. In addition, soil pHs in all P-treated plots were close to those in the control soil one year after P application, though still slightly lower. Initial low pH induced by H_3PO_4 would favor dissolution of soil Pb (*8*). Reduction of soil pH was expected with addition of H_3PO_4; however, care should be exercised when applying H_3PO_4 due to enhanced mobility of P and other heavy metals (*21*).

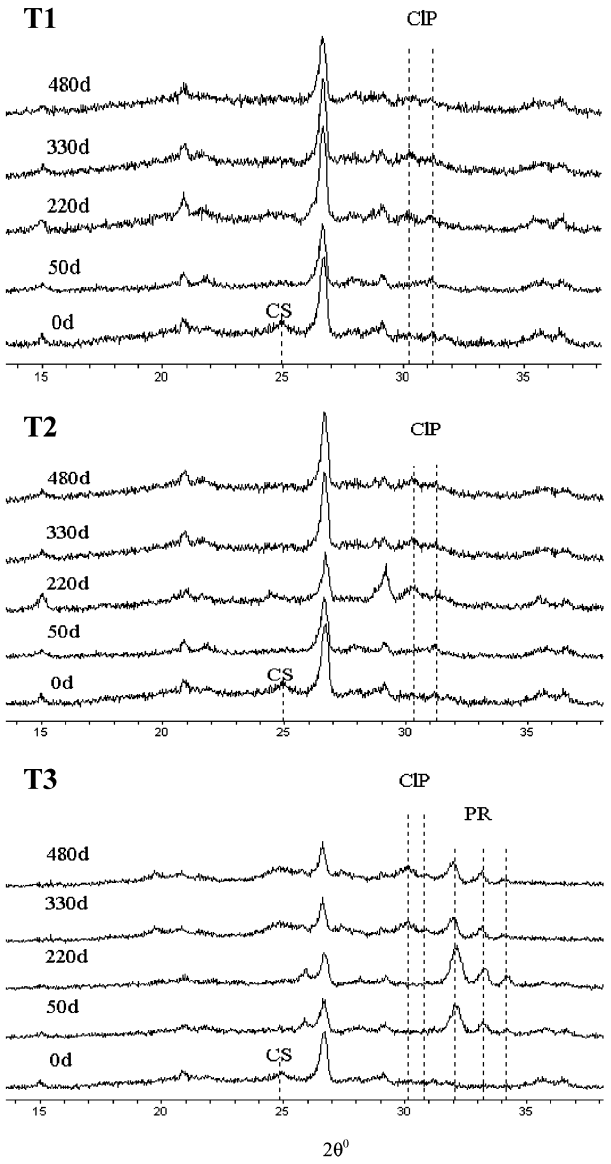

FIGURE 2. X-ray diffraction patterns of the clay fractions from surface soils (0−10 cm) in P-treated plots as a function of time. T1, T2, and T3 are the same as in Figure 1. CS, Cerussite; CIP, Chloropyromorphite; PR, Phosphate rock.

Mineralogical Analysis for the P-Treated Soils. Analysis of mineralogical changes over time resulting from P addition using XRD helps to better understand the mechanisms of Pb immobilization in the soils (Figure 2). Of the three most prominent peaks of chloropyromorphite [$Pb_{10}(PO_4)_6Cl_2$], two can be seen at 2.96 and 2.87 Å in T1 (H_3PO_4) and T2 [H_3PO_4 + $Ca(H_2PO_4)_2$] treated soil after 220 days of P application, indicating that less soluble chloropyromorphite mineral was formed in situ in these soils. For T3 (H_3PO_4 + PR) treated soil, formation of chloropyromorphite took a longer time since PR is less soluble than H_3PO_4 or $Ca(H_2PO_4)_2$. Chloropyromorphite was not observed in T3 soil until after 330 days. Note that no fluorpyromorphite [$Pb_{10}(PO_4)_6F_2$] was found in the T3 although F is a constituent of PR. Formation of chloropyromorphite instead of fluorpyromorphite in PR treated soil is expected since the former has lower solubility. Previous studies (*11, 20, 29*) showed that chloropyromorphite is present in old mine fields.

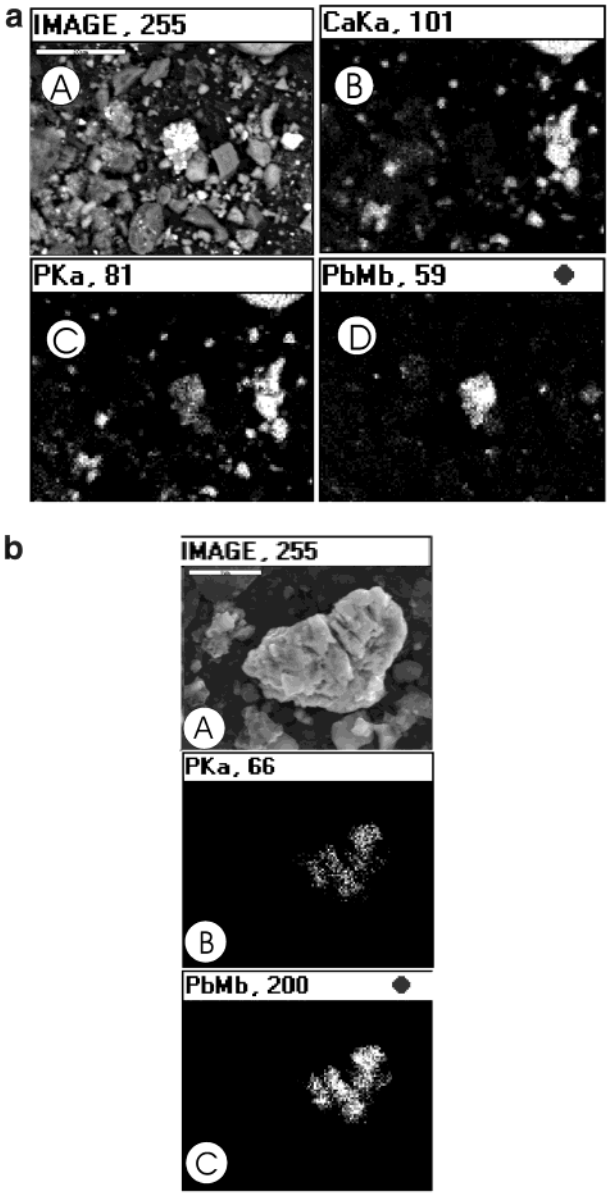

FIGURE 3. Scanning electron microscopy element dot maps of (a) T2 surface soil (0−10 cm), (A) chloropyromorphite crystal, (B) Ca, (C) P, (D) Pb, Scale bar = 20 μm; and (b) subsurface soil (30−40 cm) taken from T2 plot 330 days after P application. T2, H_3PO_4 + $Ca(H_2PO_4)_2$, (A) chloropyromorphite crystal, (B) P, (C) Pb, Scale bar = 5 μm.

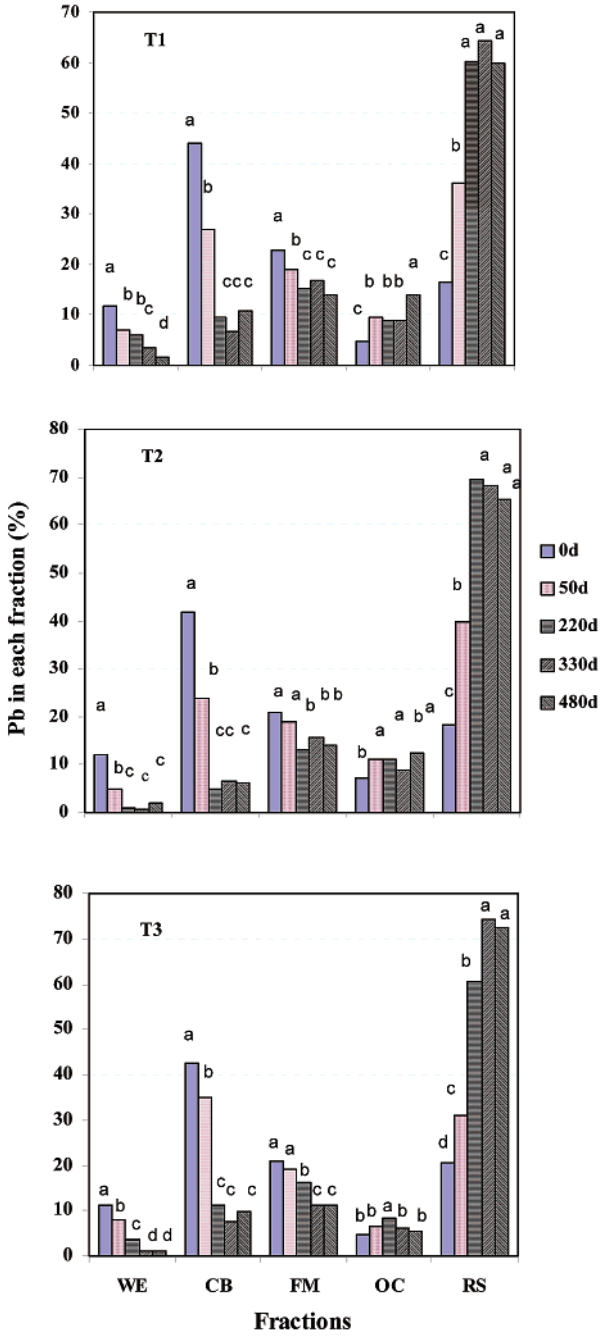

FIGURE 4. Pb distribution in T1, T2, and T3 treated surface soils (0−10 cm) as a function of time. T1, T2, and T3 are the same as in Figure 1. WE, water-soluble and exchangeable; CB, carbonate; FM, Fe−Mn oxides; OC, organic; RS, residual. Columns with the same letter within a fraction are not significantly different at $p < 0.05$.

Formation of chloropyromorphite after P addition was further evidenced by a SEM elemental dot map (Figure 3a), which showed the association of Pb with P in a soil sample taken at day 330 from T2 plot. The results were similar for T1 and T3 (data not shown). The efficiency of P treatments to immobilize Pb continued in the subsurface soil. SEM elemental dot map of a soil sample taken from 30 to 40 cm of T2 plot showed the association of Pb with P in the subsurface soil (Figure 3b). It may result from downward movement of P added as H_3PO_4 or $Ca(H_2PO_4)_2$. These results confirm that Pb immobilization can be achieved at a significant depth in a soil profile.

The peak at 2.96 Å in T1 and T2 soils was highest after day 220, suggesting that more chloropyromorphite minerals were formed between 50 and 220 days. It was worthwhile to note that in T3, the intensities of the PR peaks (between 2.70 Å and 2.80 Å) on days 330 and 480 were lower compared to the same peaks on days 50 and 130. The reduced peak intensity of PR with time might indicate further dissolution of PR. Formation of chloropyromorphite in this study occurred slowly in contrast to typical laboratory incubation results. Rabinowitz (*15*) reported that no difference was observed after 1, 3, or 7 d of incubation of contaminated soil with P, where P and Pb are generally subjected to vigorous shaking. It implied that the reaction between P and soil Pb is essentially complete in a day. However, formation of chloropyromorphite in this field study took longer since P was applied using a passive method of mixing where P is relatively less well mixed with Pb than in a laboratory setting. Also, low liquid-to-solid ratio (L/S = 0.03) at the site determined that diffusion was probably the operative

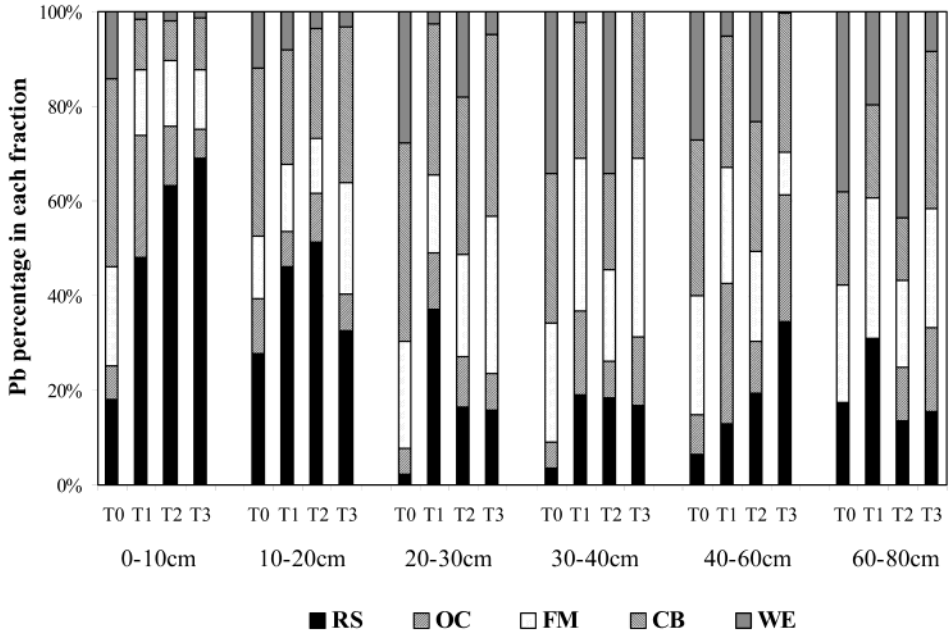

FIGURE 5. Pb distribution in the soil profile (0−80 cm) 480 days after P application. T1, T2, and T3 are the same as in Figure 1. WE, CB, FM, OC, and RS are the same as in Figure 4.

transport mechanism, causing a relatively long conversion time. Once chloropyromorphite was formed, it is relatively stable since no changes in the XRD peaks (2.96 Å) were observed in P-treated soils after 330 days (Figure 2).

Coupled with formation of chloropyromorphite, H_3PO_4-induced dissolution of cerussite, the main form of Pb at the site (Figure 2), was also evident as indicated by the disappearance of the peaks at 3.56 Å for soil samples taken from T1 to T3 (Figure 2). Our data are consistent with the hypothesis that P-induced Pb immobilization was mainly through a dissolution-precipitation mechanism (*16*).

Lead Distribution in P-Treated Soils. Chemical fractionation has been used to evaluate the efficacy of decontamination treatment (*7*, *14*). Assuming the nonresidual metal (sum of the exchangeable, carbonate, Fe−Mn oxides, and organic fraction) is more bioavailable than the residual metal, then the effectiveness of in situ remediation of metal contaminated soils can be assessed with more effective treatments converting greater amounts of metal from the nonresidual to the residual fraction or from more to less bioavailable forms (*30*).

Before P treatment (day 0), lead in the contaminated soils was primarily associated with the CB fraction (42.5−44.5%), followed by FM > RS > WE > OC (Figure 4). The sum of Pb associated with the WE and CB fractions accounted for over 50% of the total Pb, which indicated that a substantial quantity of Pb in the contaminated soil may be available for plant uptake. Xian (*31*) found the sum of Pb associated with WE and CB bound forms were strongly correlated with Pb uptake by cabbage (*Brassica oleracea*) and kidney bean (*Phaseolus vulgaris L.*) plants. Addition of phosphate to the soil significantly reduced the first three fractions (WE, CB and FM) and significantly increased the RS fraction along with a slight increase in OC Pb (Figure 4). Phosphate treatments increased residual Pb by 19−48%, 22−50%, and 11−55% for T1, T2, and T3, respectively, implying that all P treatments were able to modify the partitioning of Pb from the nonresidual/potentially available phase to the residual/unavailable phase. In this respect, the major transformation was a decrease of the CB−Pb by up to ~40%, while the residual phase was increased by up to 55%, consistent with the designed strategy of dissolving cerussite with phosphoric acid, allowing for the precipitation of geochemically stable pyromorphite (*6*). A significant decrease of Pb in the WE+CB fractions should reduce Pb bioavailability.

Conversions of nonresidual to residual Pb occurred gradually with time (Figure 4). On day 50, residual Pb increased by 20%, 22% and 11% for T1, T2, and T3, respectively, not enough for lead phosphate to be detected by XRD (Figure 2). The conversions did level off by 220 days for T1 and T2, as well as by 330 days for T3 (Figure 4). This is probably because half of the P in T3 was added as PR, which slowed the dissolution of cerussite and precipitation of chloropyromorphite due to its low solubility compared to H_3PO_4 and $Ca(H_2PO_4)_2$. This is consistent with the XRD data (Figure 2) in that chloropyromorphite peaks for T3 were not observed until day 330. It was possible that some of the Pb transformation from the nonresidual to residual may have occurred during the extraction process (*7*). However, the fact that residual Pb in all P-treated soil increased with time (Figure 4) strongly demonstrated that conversion of soil Pb to more stable forms actually occurred in the field. Therefore, a sequential extraction scheme can be effectively used to evaluate the effectiveness of P amendment to immobilize Pb in a contaminated soil.

Among the three P treated soils, PR (T3) was most effective in converting Pb from the nonresidual to residual fraction (to 74%), while the H_3PO_4 treatment (T1) was the least effective (<64%). It was possible that Pb could be adsorbed on the nondissolved fraction of PR in addition to formation of chloropyromorphite. Similarly, Hettiarachchi et al. (*32*) also reported that PR was more effective than triple superphosphate or phosphoric acid in reducing Pb bioavailability for the Zn−Pb contaminated soils in their experiment.

Phosphate was not only effective in modifying Pb distribution in the surface soil but also in the subsurface soil. Phosphate converted Pb from nonresidual to residual fraction throughout the soil profile except at depth of 60−80 cm (Figure 5). It is possibly attributable to the H_3PO_4 migration down. At the 30−40 cm depth, Pb in the residual fraction increased from 4.5% to 17−19% in the P-treated soils relative to the control. This immobilization was also demonstrated by the close association of Pb with P as shown in SEM dot map of 30−40 cm deep soil in T2 (Figure 3b).

Lead Activity Controlling Minerals. The activity-ratio diagram can describe and qualitatively interpret mineral

TABLE 2. Equilibrium Reactions for Lead Minerals and Complexes at 25 °C

mineral	equilibrium reaction	logK^{0} [a]
anglesite	$PbSO_4 \leftrightarrow Pb^{2+} + SO_4^{2-}$	−7.79
cerussite	$PbCO_3 + 2H^+ \leftrightarrow Pb^{2+} + CO_2(g) + H_2O$	4.65
$PbHPO_4$	$PbHPO_4 + H^+ \leftrightarrow Pb^{2+} + H_2PO_4^-$	−4.25
hydroxypyromorphite	$Pb_5(PO_4)_3OH + 7H^+ \leftrightarrow 5Pb^{2+} + 3H_2PO_4^- + H_2O$	−4.14
chloropyromorphite	$Pb_5(PO_4)_3Cl + 6H^+ \leftrightarrow 5Pb^{2+} + 3H_2PO_4^- + Cl^-$	−25.05

[a] Data from ref *33*.

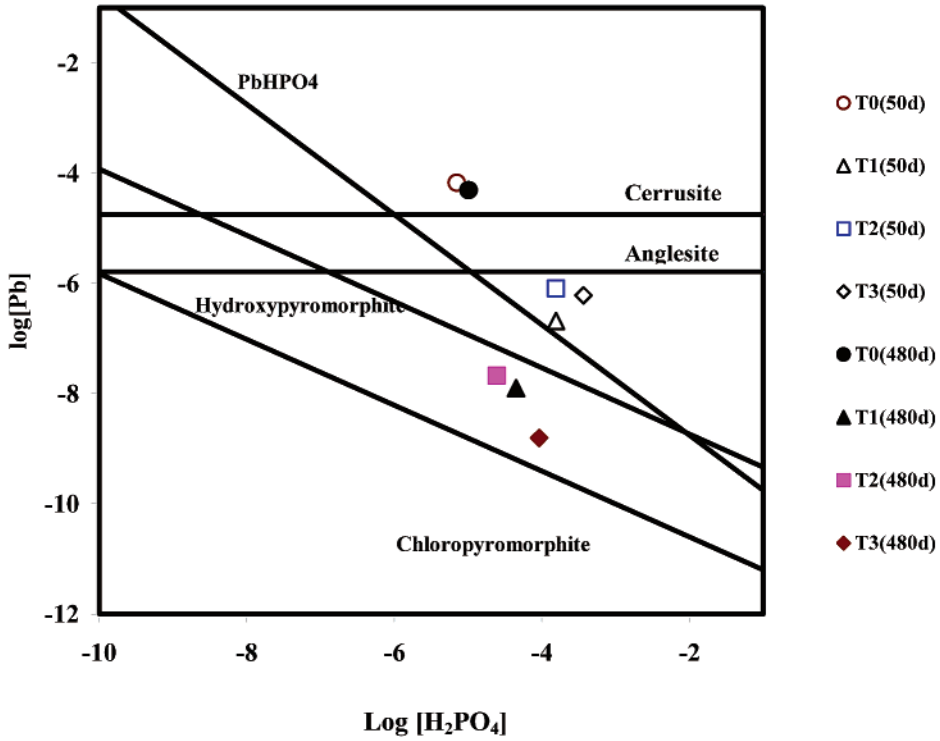

FIGURE 6. Lead activity-ratio diagram at 25 °C with soil speciation data. Plotted lines assume [Cl^-] = 10^{-4} M, [SO_4^{2-}] = 10^{-3} M, [H^+] = $10^{-6.5}$ M, and [$CO_2(g)$] = $10^{-3.5}$ M. T0, control; T1, T2, and T3 are the same as in Figure 1.

solubility data to determine potential minerals controlling metal solubility and their relative solubility (*34*). Potential Pb minerals and complexes used in the model Visual MINTEQ and the Pb activity-ratio diagram were listed in Table 2. In the current study, plotted lines assume [Cl] = 10^{-4} M, [SO_4] = 10^{-3} M, which was determined based on the average of the tested plots. According to the Pb activity ratio diagram (Figure 5), Pb solubilities decreased in the following order: $PbCO_3$ > $PbSO_4$ > $PbHPO_4$ > $Pb_5(PO_4)_3OH$ > $Pb_5(PO_4)_3Cl$ in the range of 10^{-5}−10^{-2} mol $H_2PO_4^-$ L^{-1}. For the control (T0), modeled Pb^{2+} activities were supersaturated with regard to cerussite respective of day 50 or day 480 (Figure 6). It indicated that cerussite may control Pb solubility in the soils without P treatments, in agreement with the data of XRD patterns (Figure 2). However, P treatments reduced Pb^{2+} activities. On day 50 Pb^{2+} was supersaturated with less soluble $PbHPO_4$ in all P-treated soils, showing that $PbHPO_4$ controlled Pb solubility. Pb activity in the P-treated soils decreased with time and was supersaturated with chloropyromorphite in all P-treated soils on day 480. These results agreed with XRD data (Figure 2) in that chloropyromorphite were not found until 220 days for T1 and T2 as well as 330 days for T3. Lead phosphate has been recognized as a mineral controlling Pb solubility in many P-amended soils (*19, 35*).

Phosphorus Distribution in the P-Treated Soil Profile. Since the treatment plots were exposed to rainfall, soil P enrichment and leaching may be an environmental concern for in situ Pb immobilization using P amendments. Soluble P sources (e.g. H_3PO_4, KH_2PO_4) pose a high risk of enhanced P eutrophication, while less soluble P sources (e.g. apatite, PR) pose less. Hettiarachchi et al. (*32*) reported that Bray-1 extracted much more P in triple super phosphate treated soils than in PR treated soils. Therefore, it is important to evaluate P distribution when phosphate was used to immobilize Pb in a field test from the viewpoint of potential secondary contamination of P and P utilization efficiency.

Figure 7 illustrated the P retention in the surface and profile soil of three P-treated plots as a function of time. Phosphorus in all treatments was mainly present in the surface with 45−55%, 52−65%, and 72−77% of added P for T1, T2, and T3 (Figure 7a). T3 kept more P in the surface soil than T1 and T2. A significant decrease of P was observed for T1 and T2 between 50 and 220 days. However, slight changes occurred over time for all P treatments after 220 days, especially for the PR application, indicating that most of the P loss occurred within the first 220 d in the surface soil.

As expected, downward migration of P was observed in this soil with low buffering capacity (Table 1), and this movement accounts for Pb immobilization in subsurface soil (Figure 3b). On day 50 after first P application there was no significant difference of P loss between the treatments with >94% of added P remaining in the soil profile (0−80 cm). Comparable with surface P, a significant loss of profile P occurred between 50 and 220 days, and profile P, especially in T1 and T2 treatments, decreased with the time (Figure

TABLE 3. Pb Concentration in the St. Augustine Grass (*Stenotaphrum secundatum*) Grown in the Control and P-Treated Plots

	shoots (mg kg^{-1} DW)			roots (mg kg^{-1} DW)		
	220 day	330 day	480 day	220 day	330 day	480 day
T0	77 ± 6.24a	55 ± 6.55bc	75 ± 4.58a	113 ± 23.2h	140 ± 22.5gh	202 ± 40.1 g
T1	43 ± 4.35cd	20 ± 4.35f	52 ± 3.46bc	356 ± 47.8d	444 ± 18.7c	223 ± 28.7ef
T2	62 ± 7.81b	39 ± 6.00de	56 ± 9.53b	981 ± 91.0a	600 ± 45.8b	360 ± 29.8d
T3	43 ± 8.88cd	30 ± 9.00ef	22 ± 5.19f	289 ± 24.4e	110 ± 10.5h	158 ± 19.9gh

[a] Mean ± SD ($n = 3$) with the same letter in the same part of grass are not significantly different at $p < 0.05$. T0, control; T1, H_3PO_4; T2, H_3PO_4 + $Ca(H_2PO_4)_2$; T3, H_3PO_4 + phosphate rock.

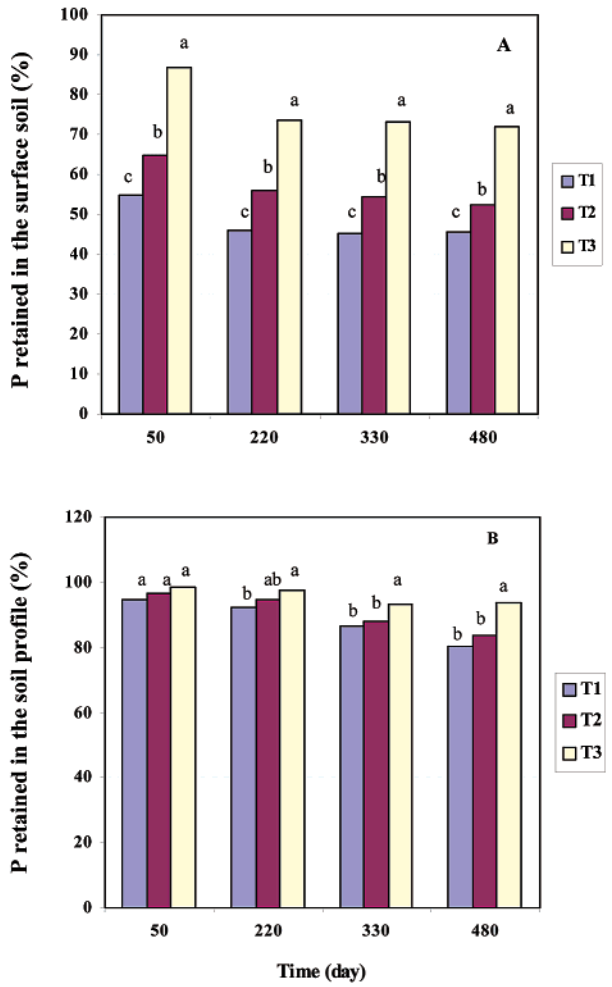

FIGURE 7. Phosphorus retained in the surface (0−10 cm) (a) and soil profile (0−80 cm) (b) from P-treated plots as a function of time. T1, T2, and T3 are the same as in Figure 1. Columns with the same letter within a time are not significantly different at $p < 0.05$.

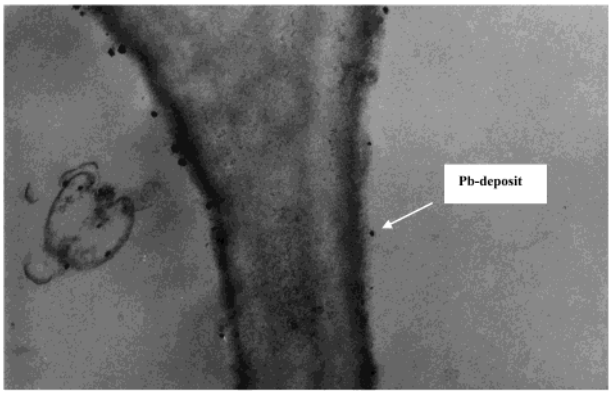

FIGURE 8. Transmission electron microscopy of Pb deposit on the cell wall of St. Augustine grass (*Stenotaphrum secundatum*) grown in T2 P-treated soil taken on 480 days after P application. T2, H_3PO_4 + $Ca(H_2PO_4)_2$. Magnification: 20 000.

7b). Approximately 93−99% of the added P remained in the soil in treatments T3, while 80−94% and 84−97% of added P remained in treatments T1 and T2, respectively. The fact that less P downward movement and less P loss in the T3 than T1 and T2 indicates that PR treatment poses the least risk of eutrophication to the environment and provides more P to react with Pb in the soil.

Effects of P Application on Pb Phytoavailability. Three cuttings of the grass were collected at 220, 330, and 480 days and analyzed for total Pb (Table 3). Aboveground biomass regenerated from the roots after each cutting. Theoretically, successive removal of the grass biomass from the soil would reduce Pb in both roots and shoots with cutting. This was true for the roots in which Pb concentrations in the control and treatments decreased with time ($p < 0.05$) but not for the shoots except in T3 ($p < 0.05$) (Table 3). It may be because the grass was naturally growing at the site before P amendments, so Pb uptake by plants varied with the growth phases. Optimization of the growing conditions may result in an increased yield without decreasing metal concentrations in the plant (*36*). It was difficult to compare the biomass among treatments since there was biomass difference before P application because the grass was naturally growing on the site.

Nevertheless, shoot tissue Pb contents decreased significantly ($p < 0.05$) after P amendment with reduction of 31−64%, 20−29%, and 44−71% for T1, T2, and T3, respectively, relative to the control T0. Similar results were obtained in the previous investigations that tissue Pb concentrations in maize (*Zea mays*), barley (*Hordeum vulgare*), and sudax (*Sorghum bicolor L. Moench*) were reduced after application of P to Pb polluted soils (*25, 37*). However, the Pb concentration in the plant roots was elevated in all P-treated plots except treatment T3 in which Pb concentrations in the roots were ≤ the control after 330 and 480 d, respectively (Table 3). Similar results were observed by Laperche et al. (*25*) who reported that when adding high quantities of P to a Pb contaminated soil, the content of Pb in the plant roots was ≥ the unamended soil. It is likely that P uptake enhanced Pb uptake, probably due to improved plant nutrition. It was found that Pb uptake in the roots was positively correlated with P ($r = 0.84$, $p < 0.05$). In addition, H_3PO_4 addition possibly resulted in a temporary increase in Pb activity in the soil. Note, elevation of Pb in the root seemly contradicted with Pb reduction in 0.01 M $Ca(NO_3)_2$ extract after P treatment (Figure 6). However, Pb uptake is related to soil Pb phytoavailability. Different chemical forms of Pb have different availability. Therefore, Pb reduction in 0.01 M $Ca(NO_3)_2$ extract does not necessarily mean Pb uptake reduction.

It is conceivable that interactions between heavy metals and P may occur in plants similarly to those known to occur in the soil (*38*). Consequently, we hypothesized that Pb was accumulated inside the root or on the root surface as lead phosphate. Thus, less translocation of lead would occur from the root to shoot, reducing shoot Pb concentrations. The

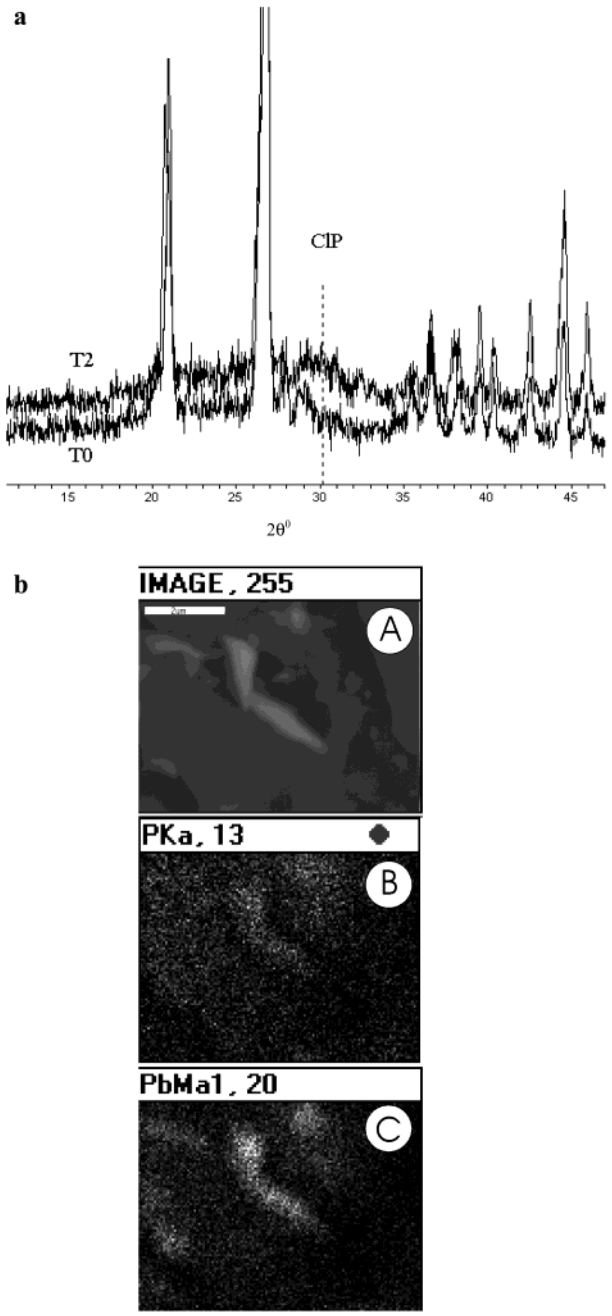

FIGURE 9. X-ray diffraction patterns (a) and scanning electron microscopy element dot map (b) of a root rhizosphere soil in T2 plot taken on 480 days after P application. CIP, Chloropyromorphite. (A) chloropyromorphite crystal, (B) P, (C) Pb, Scale bar = 2 μm.

hypothesis was supported by TEM evidence of roots grown in T2 treated plot that showed Pb deposited on root cell walls of roots (Figure 8). Furthermore, EDS showed association of Pb with P (data not shown), indicating that formation of a lead phosphate occurred in the roots. Similarly, others reported that analysis of a root section by TEM showed Pb−P deposited next to root cell walls grown in hydroxyapatite or PR treated soils (*25*). The exact mineralogical identity of the Pb deposit in the root is under further study.

Another possible explanation for chloropyromorphite formation in the rhizosphere may be that plant roots created local acidity, which may have enhanced the local dissolution of apatite grains and precipitation of pyromorphite on the root surface (*18*, *38*). The association of pyromorphite with the outermost layer of root cells and the contribution of root exudates in pyromorphite formation were found by Cotter-Howells (*38*). XRD patterns indicated a peak of chloropyromorphite at approximately 2.97 Å in the rhizosphere soil from the T2 amendment (Figure 9a) which was absent in the control. Also, SEM examination showed that Pb was associated with P (Figure 9b). Therefore, formation of a Pb−P precipitate within the root rhizosphere and in the bulk soil after P application would be responsible for the reduced translocation of Pb from the roots to the shoots and therefore a reduction of Pb concentration in the above-ground biomass.

Based on our field results, P amendments were effective in reducing Pb mobility via in situ formation of insoluble chloropyromorphite minerals in the field. The formation of chloropyromorphite in the soils and on the root cell wall of St. Augustine grass were responsible for decreasing lead translocation from the roots to shoots, thereby reducing shoot Pb concentration. A mixture of H_3PO_4 and phosphate rock was most effective for Pb immobilization, with the least impact on soil pH, and posing the lowest eutrophication risk. For more efficient Pb immobilization, pH reduction using H_3PO_4 became necessary to dissolve carbonate-bound Pb and make Pb readily available for the geochemically stable Pb phosphate formation. We conclude that combined H_3PO_4 with phosphate rock application can be more effectively used to immobilize Pb in contaminated soils, thus offering an alternative technology for phosphate to remediate contaminated sites. However, caution should exercised to maximize lead immobilization and minimize potential adverse impacts caused by application of phosphate amendments to soils.

Acknowledgments

This research was supported in part by the Florida Institute of Phosphate Research (Contract No. 97-01-148R). The authors would like to thank Mr. Thomas Luongo for his assistance in chemical analysis and in proof-reading the manuscript. We also thank Wayne Acree, Karen Kelley, and Eric Fodran for their help in electron microscopy analysis.

Literature Cited

(1) Nedwed, T.; Clifford, D. A. *Waste Manage.* **1997**, *17*, 257−269.
(2) Basta, N. T.; Gradwohl, R.; Snethen, K. L.; Schroder, J. L. *J. Environ. Qual.* **2001**, *30*, 1222−1230.
(3) Boisson, J.; Ruttens, A.; Mench, M.; Vangronsveld, J. *Environ. Pollut.* **1999**, *104*, 225−233.
(4) Cotter-Howells, J.; Caporn, S. *Appl. Geochem.* **1996**, *11*, 335−342.
(5) Hettiarachchi, G. M.; Pierzynski, G. M.; Ransom, M. D. *Environ. Sci. Technol.* **2000**, *34*, 4614−4619.
(6) Ma, L. Q.; Logan, T. J.; Traina, S. J. *Environ. Sci. Technol.* **1995**, *29*, 1118−1126.
(7) Ryan, J. A.; Zhang, P.; Hesterberg, D.; Chou, J.; Sayers, D. E. *Environ. Sci. Technol.* **2001**, *35*, 3798−3803.
(8) Yang, J.; Mosby, D. E.; Casteel, S. W.; Blancher, R. W. *Environ. Sci. Technol.* **2001**, *35*, 3553−3559.
(9) Laperche, V.; Traina, S. J.; Gaddam, P.; Logan, T. J. *Environ. Sci. Technol.* **1996**, *30*, 3321−3326
(10) Ruby, M. V.; Davis, A.; Nicholson, A. *Environ. Sci. Technol.* **1994**, *28*, 646−654.
(11) Cotter-Howells, J. D.; Thornton, I. *Environ. Geochem. Health* **1991**, 127−135.
(12) Davis, A. P.; Hotha, B. V. *J. Environ. Eng.* **1998**, 1066−1075.
(13) Cotter-Howells, J. *Environ. Pollut.* **1996**, *93*, 9−16.
(14) Berti, W. R.; Cunningham, S. D. *Environ. Sci. Technol.* **1997**, *31*, 1359−1364.
(15) Rabinowitz, M. B. *Bull. Environ. Contam. Toxicol.* **1993**, *51*, 438−444.
(16) Ma, Q. Y.; Traina, S. J.; Logan, T. J. *Environ. Sci. Technol.* **1993**, *27*, 1803−1810.
(17) Lower, S. K.; Maurice, P. A.; Traina, S. J. *Geochim. Cosmochim. Acta* **1998**, *62*, 1773−1780.
(18) Traina, S. J.; Laperche, V. *Proc. Natl. Acad. Sci. U.S.A.* **1999**, *96*, 3365−3371.
(19) Christensen, T. H.; Nielsen, B. G. Retardation of Lead in Soil. In *Heavy Metals in the Environment*; CEP Consultants: Edinburgh, 1987; pp 319−321

(20) Eusden, J. D.; Gallagher, L.; Eighmy T. T.; Crannell, B. S.; Krzanowski, J. R.; Butler, L. G.; Cartledge, F. K.; Emery E. F.; Shaw, E. L.; Francis, C. A. *Waste Manage.* **2002**, *22*, 117−135.
(21) Cao, X.; Ma, L. Q.; Singh, S. P.; Chen, M.; Harris, W. G.; Kizza, P. *Field Demonstration of Metal Immobilization in Contaminated Soils Using Phosphate Amendments*; Final Report to the Florida Institute of Phosphate Research; University of Florida: Gainesville, FL, 2001; pp 5−33
(22) Tessier, A.; Campbell; P. G. C.; Bisson, M. *Anal. Chem.* **1979**, *51*, 844−851.
(23) Gustaffsson, J. P. http://amov.ce.kth.se/PEOPLE/gustafjp/vminteq2.htm (verified Aug. 6, 2001).
(24) Klute, A. *Methods of Soil Analysis, Part 1 Physical and Mineralogical Methods*, 2nd ed.; ASA: Madison, WI, 1986; Vol. 9, pp 331−349.
(25) Laperche, V.; Logan, T. J.; Gaddam, P.; Traina, S. *Environ. Sci. Technol.* **1997**, *31*, 2745−2753.
(26) Page, A. L.; Miller, R. H.; Keeney, D. R. *Methods of Soil Analysis, Part 2 Chemical and Microbiological Properties*, 2nd ed.; ASA: Madison, WI, 1982; Vol. 9, pp 539−577.
(27) Page, A. L.; Miller, R. H.; Keeney, D. R. *Methods of Soil Analysis, Part 2 Chemical and Microbiological Properties*, 2nd ed.; ASA: Madison, WI, 1982; Vol. 9, pp 149−157.
(28) Page, A. L.; Miller, R. H.; Keeney, D. R. *Methods of Soil Analysis, Part 2 Chemical and Microbiological Properties*, 2nd ed.; ASA: Madison, WI, 1982; Vol. 9, pp 403−427.
(29) Cotter-Howells, J.; Champness, P. E.; Charnock, J. M.; Pattrick, R. A. D. *Eur. J. Soil Sci.* **1994**, *45*, 393−399.
(30) Ma, L. Q.; Choate, A. L.; Rao, G. N. *J. Environ. Qual.* **1997**, *26*, 801−807.
(31) Xian, X. *Plant Soil* **1989**, *113*, 257−264.
(32) Hettiarachchi, G. M.; Pierzynski, G. M.; Ransom, M. D. *J. Environ. Qual.* **2001**, *30*, 1214−1221.
(33) Lindsay, W. L. *Chemical Equilibria in Soils*; John Wiley & Sons: New York 1979; pp 329−341.
(34) McGowen, S. L.; Basta, N. T.; Brown, G. O. *J. Environ. Qual.* **2001**, *30*, 493−500.
(35) Santillian-Medrano, J.; Jurinak, J. J. *Soil Sci. Soc. Am. Proc.* **1975**, *39*, 851−856.
(36) Lombi, E.; Zhao, F. J.; Dunham, S. J. *J. Environ. Qual.* **2001**, *30*, 1919−1926.
(37) Chlopecka, A.; Adriano, D. C. *Sci. Total Environ.* **1997**, *207*, 195−206.
(38) Cotter-Howells, J. D.; Champness, P. E.; Charnock, J. M. *Mineral. Mag.* **1999**, *63*, 777−789.

Received for review April 19, 2002. Revised manuscript received September 23, 2002. Accepted September 25, 2002.

ES020697J